ERDC/CERL TR-00-1

Construction Engineering Research Laboratory

US Army Corps of Engineers®
Engineer Research and Development Center

Bus Current Feedback for Motor Control

by Hannon T. Maase, Jonathan A. Locker,
and Philip T. Krein

January 2000

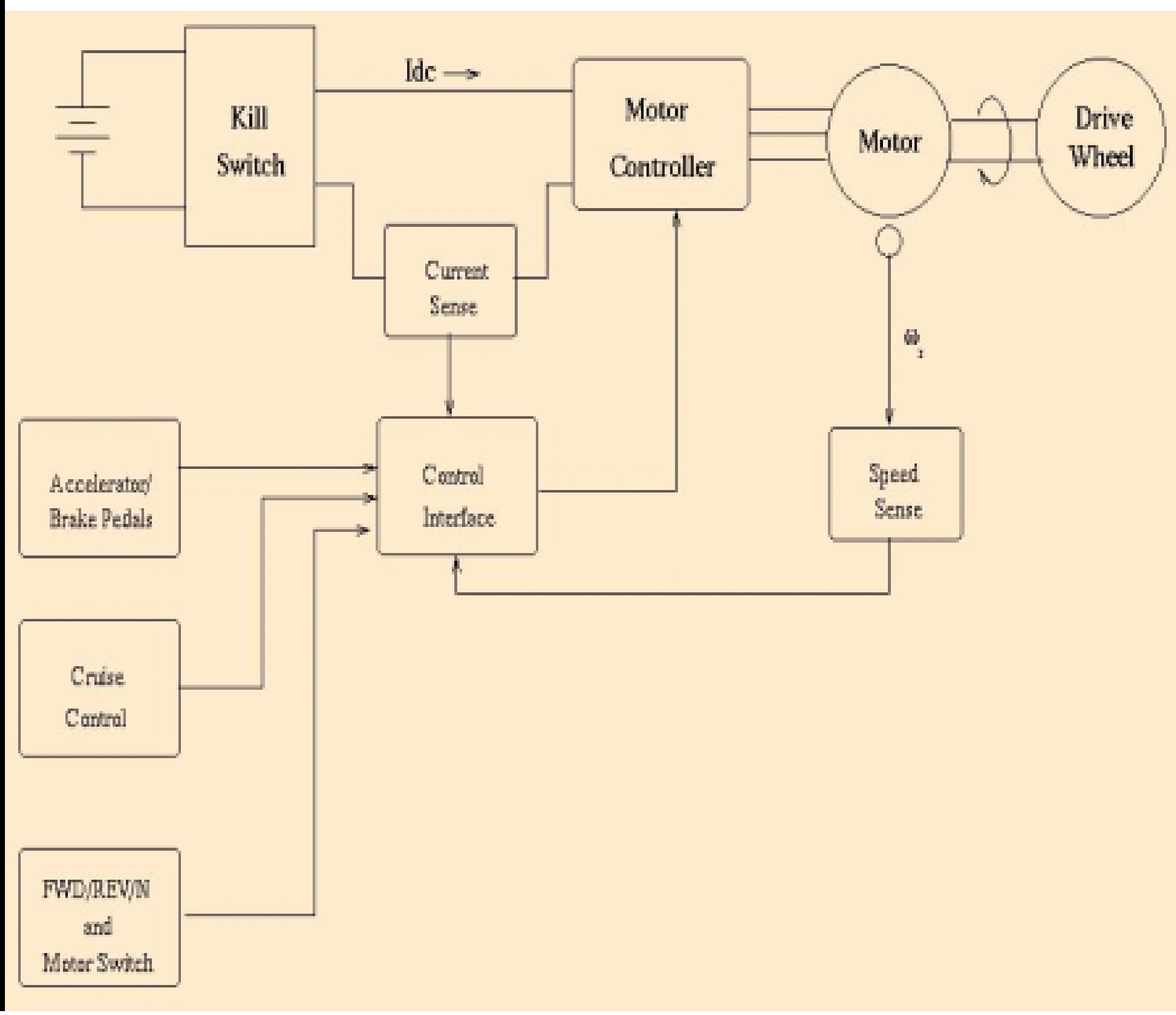

Foreword

This study was conducted under the Inter-Laboratory Independent Research (ILIR) program. The work was performed by the Energy Branch (CF-E), of the Facilities Division (CF), U.S. Army Construction Engineering Research Laboratory (CERL). Jonathan A. Locker and Philip T. Krein are associated with the Department of Electrical and Computer Engineering, University of Illinois, Urbana-Champaign (UIUC). The CERL principal investigator was Hannon T. Maase. Larry M. Windingland is Chief, CEERD-CF-E, and L. Michael Golish is Chief, CEERD-CF. The technical editor was William J. Wolfe, Information Technology Laboratory – CERL. The Acting Director of CERL is Dr. Alan W. Moore.

CERL is an element of the U.S. Army Engineer Research and Development Center (ERDC), U.S. Army Corps of Engineers. The Acting Director of ERDC is Dr. Lewis E. Link and the Commander is COL Robin R. Cababa, EN.

Contents

List of Figures

Figures

1 Introduction

Background

In recent years, a number of algorithms using new nonlinear control ideas have been applied to the induction motor control problem. Many of these algorithms allow the user to control the torque, speed, or position response of a closed loop servo quite precisely, but such methods require precise knowledge of motor parameters and a great deal of computational power. For many applications, the incremental improvement in transient torque, speed, or position response does not justify the additional computational requirements or a complicated tuning and commissioning process. A better solution would be to improve the utility of existing algorithms that may normally exhibit lower performance, but that can be extended easily.

One such extension involves the use of the DC link current as a control variable in various motor control algorithms. This work examined the use of such a variable as an enhancement for scalar and vector control algorithms for the induction motor. Further, some of the effects of such a control on the operation of an electric vehicle were also presented and discussed.

Objective

The objective of this research was to examine the use of the DC link current as a control variable in various motor control algorithms as an enhancement for scalar and vector control algorithms.

Approach

This conceptual study began with a literature search into the area of non-linear control. A mathematical model was developed and applied to a simulation study involving a solar vehicle drive system.

Mode of Technology Transfer

It is also anticipated that the results of this work will be made publicly available through CERL's world wide web (WWW) page at URL:

http://www.cecer.Army.mil

2 Control Algorithms

Eq 1 gives a mathematical model describing the operation the induction motor is given in. The motor is represented by a fifth order, nonlinear system with parameters such as inductances and resistances. For the purposes of this research, the model was taken to be representative of motor operation over the full range of interest. This assumes that nonlinear phenomena such as magnetic saturation and the time dependence of certain parameters are not included. Such assumptions are conventional in motor control design. The motor state variables include the stator currents, rotor magnetic fluxes, and rotor speed. The stator current and rotor flux variables are represented in a dq0 reference frame as per Park's transformation (Krause 1986). The motor input is the two-dimensional stator voltage variable (vds, vqs).

$$
\begin{aligned}
\frac{d}{dt} i_{ds} &= \gamma\, i_{ds} + \omega\, i_{qs} + \frac{M\, r_r}{\sigma\, L_r^2} \lambda_{dr} + \frac{M\, n_p\, \omega_r}{\sigma\, L_r} \lambda_{qr} + \frac{v_{ds}}{\sigma} \\
\frac{d}{dt} i_{qs} &= \omega\, i_{ds}\, \gamma\, i_{qs} \frac{M\, n_p\, \omega_r}{\sigma\, L_r} \lambda_{dr} + \frac{M\, r_r}{\sigma\, L_r^2} \lambda_{qr} + \frac{v_{qs}}{\sigma} \\
\frac{d}{dt} \lambda_{dr} &= \frac{M\, r_r}{L_r} i_{ds} \frac{r_r}{L_r} \lambda_{dr} + (\omega\, n_p\, \omega_r)\, \lambda_{qr} \\
\frac{d}{dt} \lambda_{qr} &= \frac{M\, r_r}{L_r} i_{qs} (\omega\, n_p\, \omega_r)\, \lambda_{dr} \frac{r_r}{L_r} \lambda_{qr} \\
\frac{d}{dt} \omega_r &= \frac{3}{2} \frac{M\, n_p}{J\, L_r} (\lambda_{dr}\, i_{qs}\, \lambda_{qr}\, i_{ds}) \frac{T_l}{J}
\end{aligned}
\qquad \text{[Eq 1]}
$$

$$
\gamma\_ \frac{M^2 r_r + L_r^2 r_s}{\sigma\, L_r^2}
$$

$$
\sigma\_ \frac{L_s\, L_r\, M^2}{L_r}
$$

Scalar Control

The simplest method for controlling an induction motor is to exploit its steady-state characteristic, which exhibits a near-linear relationship between the electrical torque and slip frequency around the synchronous frequency. A controller can excite the stator with a sinusoidal waveform of constant frequency and constant magnitude, controlling each to match a dynamically changing slip frequency as required. The magnitude of the applied voltage should be sufficient to maintain the rated flux magnitude throughout the rotor. Eq 2 gives the equations for a simple scalar controller. For this controller, gain constants k_p and k_i control the dynamics of convergence and should be set to satisfy design characteristics. Besides the relationships delineated in Eq 2, several of these variables must be limited for the controller to have good characteristics. For example, the voltage magnitude V_{mag} should have both a minimum and a maximum limit to ensure that it has enough boost at low frequencies, and that it reflects the limits of the DC voltage bus at high frequencies. Also, performance can be improved slightly with additional feedback; a controller can be augmented to compensate for stator resistive loss.

$$\begin{aligned}
\omega_{err} &= \omega_{err} - \omega_r \\
\frac{dx}{dt} &= \omega_{err} \\
\omega_e &= \omega_r + k_p \omega_{err} + k_i x \\
\frac{d\theta}{dt} &= \omega_e \\
V_{mag} &= \Lambda_{rated} \omega_e \\
v_{ds} &= V_{mag} \cos(\theta) \\
v_{qs} &= V_{mag} \sin(\theta)
\end{aligned} \qquad \text{[Eq 2]}$$

Field-Oriented Control

The best known of the so-called vector control methods, *field-oriented control* (FOC) represents an algorithm that asymptotically linearizes the flux-charging and torque-producing mechanisms for motor control. Blaschke (1972) used the transformation shown in Eq 3:

$$\begin{aligned}
\Lambda_r &\doteq \sqrt{\lambda_{dr}^2 + \lambda_{qr}^2} \\
\rho &\doteq \tan^{-1}\left({}^{\lambda_{qr}}\!/\!_{\lambda_{dr}} \right) \\
\begin{bmatrix} i_d \\ i_q \end{bmatrix} &\doteq \begin{bmatrix} \cos\rho & \sin\rho \\ -\sin\rho & \cos\rho \end{bmatrix} \begin{bmatrix} i_{ds} \\ i_{qs} \end{bmatrix} \\
\begin{bmatrix} v_d \\ v_q \end{bmatrix} &\doteq \begin{bmatrix} \cos\rho & \sin\rho \\ -\sin\rho & \cos\rho \end{bmatrix} \begin{bmatrix} v_{ds} \\ v_{qs} \end{bmatrix}
\end{aligned} \qquad \text{[Eq 3]}$$

to rearrange Eq 1 into a set of asymptotically linear equations, as shown in Eq 4.

$$\begin{aligned}
\frac{d\,\Lambda_r}{dt} &= \frac{r_r}{L_r}\Lambda_r + \frac{M\,r_r}{L_r} i_d \\
\frac{d\,i_d}{dt} &= \frac{1}{\sigma}\Big(\frac{M^2 r_r}{L_r^2} + r_s\Big) i_d + \frac{M\,r_r}{\sigma\,L_r^2}\Lambda_r + n_p\,\omega_r\,i_q + \frac{M\,r_r}{L_r\,\Lambda_r} i_q^2 + \frac{v_d}{\sigma} \\
\frac{d\,i_q}{dt} &= \frac{1}{\sigma}\Big(\frac{M^2 r_r}{L_r^2} + r_s\Big) i_q \frac{M\,n_p}{\sigma\,L_r}\Lambda_r\,\omega_r\,n_p\,\omega_r\,i_d \frac{M\,r_r}{L_r\,\Lambda_r} i_q\,i_d + \frac{v_q}{\sigma} \\
\frac{d\,\omega_r}{dt} &= \frac{3}{2}\frac{M\,n_p}{J\,L_r}\Lambda_r\,i_q \frac{T_l}{J} \\
\frac{d\rho}{dt} &= n_p\,\omega_r + \frac{r_r}{L_r}\frac{M\,i_q}{\Lambda_r}
\end{aligned} \qquad \text{[Eq 4]}$$

The transformation in Eq 3 represents variables that are referenced to a reference frame attached to the rotor flux vector. The new system form in Eq 4 exhibits asymptotic decoupling. If i_d is allowed to come to steady state, the flux will become constant, and the pair of equations in (i_q, ω_r) becomes separate from the pair in (i_d, Λ_r).

The nonlinearities in Eq 4 are canceled out with feedback, as follows. We can define new inputs u_{speed} and u_{flux} such that:

$$\begin{aligned}
v_d \,_\, &\sigma\Big(u_{flux}\,n_p\,\omega_r\,i_q \frac{M\,r_r\,i_q^2}{L_r\,\Lambda_r}\Big) \\
v_q \,_\, &\sigma\Big(u_{speed} + n_p\,\omega_r\,i_d + \frac{M\,n_p}{\sigma\,L_r}\omega_r\,\Lambda_r + \frac{M\,r_r}{L_r}\frac{i_d\,i_q}{\Lambda_r}\Big)
\end{aligned} \qquad \text{[Eq 5]}$$

With this feedback and the rotor time constant $\tau_r = L_r / R_r$, the model in Eq 4 is transformed into a form similar to that of a separately excited DC motor, as in Eq 6. The field current in a DC motor is analogous to the current i_d, and the armature current is analogous to i_q.

$$\begin{aligned}
\frac{d\,\omega_r}{dt} &= \frac{3}{2}\frac{n_p\,M}{J\,L_r}\Lambda_r\,i_q \frac{T_l}{J} \\
\frac{d\,i_q}{dt} &= \gamma\,i_q + u_{speed} \\
\frac{d\,\Lambda_r}{dt} &= \frac{1}{\tau_r}(\Lambda_r + M\,i_d) \\
\frac{d\,i_d}{dt} &= \gamma\,i_d + \frac{M}{\tau_r}\Lambda_r + u_{flux} \\
\frac{d\rho}{dt} &= n_p\,\omega_r + \frac{M\,i_q}{\tau_r\,\Lambda_r}
\end{aligned} \qquad \text{[Eq 6]}$$

FOC then represents the general technique of using Eq 6 as the basis for induction motor control. This has been the topic of hundreds of papers in AC motor control. Various FOC approaches have been implemented in commercial products.

Bus Current Control

Although FOC is well known and widely applied, it has fundamental shortcomings that motivate alternatives. First, this nonlinear feedback compensation approach requires accurate values for the various motor parameters. The performance of FOC methods is sensitive to parameter error (DeDoncker 1994), and a detailed commissioning and tuning process is necessary to set up a system. Parameters such as rotor resistance, which vary with temperature and that cannot be measured directly, make the tuning process difficult. A given controller, then, is uniquely tuned for a single motor, and the process starts over if a new motor is substituted.

FOC methods also require knowledge of certain indirect state variables, notably the rotor flux magnitude and position. Magnetic sensors can be used to provide approximate values. More commonly, an estimator is used to compute values for Λ_r and ρ. The most common estimators require a rotor position sensor, and give rise to *indirect* FOC methods.

In a wide range of applications, the dynamic capabilities of FOC do not necessarily justify its limitations. Many standard motor loads such as fans, pumps, mixers, simple conveyors, and transportation drives can benefit from good control, but have modest dynamic performance specifications. In many of these cases, motor interchangeability would be a strong advantage. For these and many other applications, extensions of scalar controls are of interest.

In *bus current control*, we take advantage of the structure of a conventional variable-frequency AC drive. Such a system rectifies an incoming AC line to provide a filtered DC bus. The DC bus is used to supply an inverter, which produces the desired AC output. The DC bus acts as the direct energy link between the AC input and the motor, and information measured at the bus can be used for control. Bus current control is an approach in which the average current drawn from the DC bus by the inverter is sensed and used for feedback control. Since this current is the ratio of inverter input power to bus voltage, and since bus voltage is nearly constant (determined by the input line), the DC bus current conveys information about load power consumption. If the power lost in the inverter and motor were arbitrarily low, then DC bus current would reflect the load power. Thus DC bus current acts as an estimate of load power, and its application in a feedback controller is intended to be equivalent to load power control.

3 Analysis of Bus Current Control

The properties of bus current control become more apparent when the rotor flux reference frame transformation is applied to a system. First, it is instructive to relate the bus current to the motor state variables in Eq 1 and Eq 4. Several assumptions help clarify the relationships. The voltage bus can be taken as a constant V_{bus} — quite accurate when the input is a fixed (stiff) AC line, and still useful if a battery source serves to generate the bus. We also assume that around an operating point, we can relate the input and output electrical power, as in Eq 7:

$$P_{out} = \eta P_{in} \quad \text{[Eq 7]}$$

such that η acts as an efficiency parameter. For relative notational simplicity, also make the symbolic substitutions:

$$a \doteq \frac{3}{2}\frac{Mn_p}{JL_r} \qquad b \doteq \frac{aJ}{\eta V_{bus}} \quad \text{[Eq 8]}$$

Here the DC bus current can be related to the FOC state variables as in Eq 9:

$$I_{bus} = b\Lambda_r i_q \omega_r \quad \text{[Eq 9]}$$

This confirms that, under these assumptions, I_{bus} is indeed proportional to the output load power $T_e\omega_r$, where T_e is the electrically produced torque.

To analyze a closed-loop system in which I_{bus} is used for feedback, it can be instructive to first consider the case where the rotational inertia is very large and the flux loop dynamics are well controlled. In normal operation, the flux loop control typically brings the flux magnitude up to its rated value before the torque loop is actuated. Once this has happened, flux magnitude is just:

$$\Lambda_r = \Lambda_{rated} \quad \text{[Eq 10]}$$

and no new information can be obtained with a measurement. With high inertia, the rotational speed will remain constant and power changes will be reflected solely in the torque of electrical origin, T_e. Thus, the dynamics of the bus current are:

$$\frac{dI_{bus}}{dt} = b\Lambda_{rated}\omega_r \frac{di_q}{dt} \qquad \text{[Eq 11]}$$

In this case, bus current feedback can be implemented with a proportional-integral (PI) loop, with x_I as the integrator state variable:

$$\frac{dx_I}{dt} = I_{ref} - I_{bus} \qquad \text{[Eq 12]}$$
$$u_{speed} = k_p\left(I_{ref} - I_{bus}\right) + k_i x_I$$

With the feedback in Eq 2 applied to the system described in Eq 6, full control over the placement of poles and zeros can be achieved according to the system transfer function:

$$\frac{I_{bus}(s)}{I_{ref}(s)} = \frac{sk_p + k_i}{s^2 + \left(\gamma + k_p\right)s + k_i} \qquad \text{[Eq 13]}$$

The above analysis can largely be repeated for the case where high inertia J no longer restricts the rotational speed ω_r. Here, both dynamics must be taken into account. A closed loop transfer function can still be found by linearizing the system about a nominal operating point. The linearization is necessary because the system is no longer linear when both speed and torque changes are taken into account:

$$\frac{dI_{bus}}{dt} = ab\Lambda_r^2 i_q^2 - I_{bus}\left(\frac{k_0'}{\omega_r} + k_1' + k_2'\omega_r + \gamma\right) + \frac{k_p}{i_q} I_{bus}\left(I_{ref} - I_{bus}\right) + k_i x_I \qquad \text{[Eq 14]}$$

In Eq 14, the constants k_0, k_0, and k_0 represent the load torque coefficients as defined by:

$$T_l \doteq k_0 + k_1\omega_r + k_2\omega_r^2 \qquad \text{[Eq 15]}$$
$$\begin{bmatrix} k_0' & k_1' & k_2' \end{bmatrix} \doteq J^{-1}\begin{bmatrix} k_0 & k_1 & k_2 \end{bmatrix}$$

The closed loop system can be shown to converge through examination of the linearized system. When only the speed (and torque) loop is considered, the closed loop system is shown in Eq 16. This equation shows that about an operating point, the system dynamics can be described by a linear dynamic equation, so conventional linear design techniques can be applied:

$$\begin{aligned}
\frac{d\tilde{I}_{bus}}{dt} &= a_1''\tilde{I}_{bus} + a_2''\tilde{\omega}_r + a_3''\tilde{i}_q + a_4''\tilde{I}_{ref} \\
\frac{d\tilde{\omega}_r}{dt} &= a\Lambda_r\tilde{i}_q - k_1'\tilde{\omega}_r - 2k_2'\omega_{r0}\tilde{\omega}_r \\
\frac{d\tilde{x}_I}{dt} &= \tilde{I}_{ref} - \tilde{I}_{bus} \\
\frac{d\tilde{i}_q}{dt} &= -\gamma\tilde{i}_q + k_p\left(\tilde{I}_{ref} - \tilde{I}_{bus}\right) + k_i\tilde{x}_I
\end{aligned} \qquad \text{[Eq 16]}$$

4 Simulation Studies

Figure 1 shows a SIMULINK block diagram representing a DC bus current controller applied to a speed-controlled induction motor. In this simulation, a standard slip controller (a type of closed-loop scalar control) is augmented with current feedback. The bus current I_{dc} is calculated from the motor voltages and currents as in Eq 17. The power signal is also filtered to mimic a sensor delay as well as prevent an algebraic loop within the simulation. This simulation uses a 100 V DC bus as its voltage source.

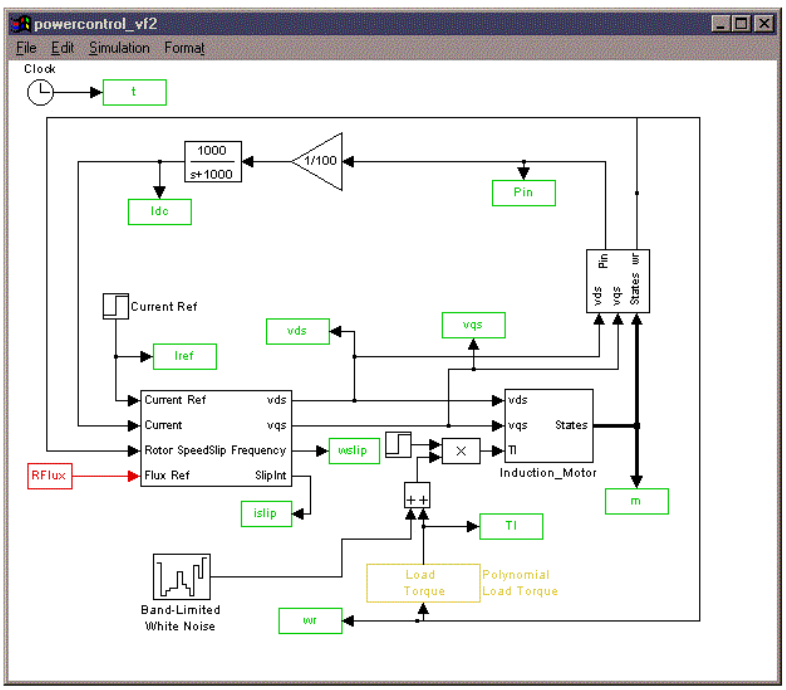

Figure 1. DC bus current loop for a scalar controller.

Figure 2 shows a block diagram of closed-loop bus current control.

$$P_{in} = \frac{3}{2}\left(v_{ds} i_{ds} + v_{qs} i_{qs}\right), \quad I_{bus} = P_{in} / V_{bus} \qquad \textbf{[Eq 17]}$$

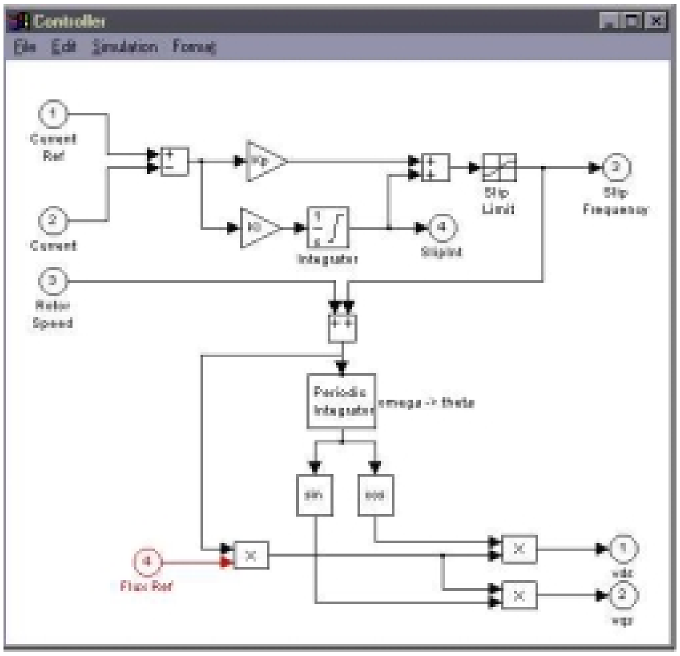

Figure 2. Bus current controller.

Figures 3 and 4 show the results from the current loop controller. In the simulation, a second-order load torque with a position-dependent disturbance component was applied after one second had elapsed. The current loop controller is able to regulate the bus current to within a few milliamps in this simulation. Furthermore, even in the presence of a fairly large load torque perturbation, the rotor speed is relatively constant. Figure 4 emphasizes this by expanding the speed error at about 10 s after the start of the simulation.

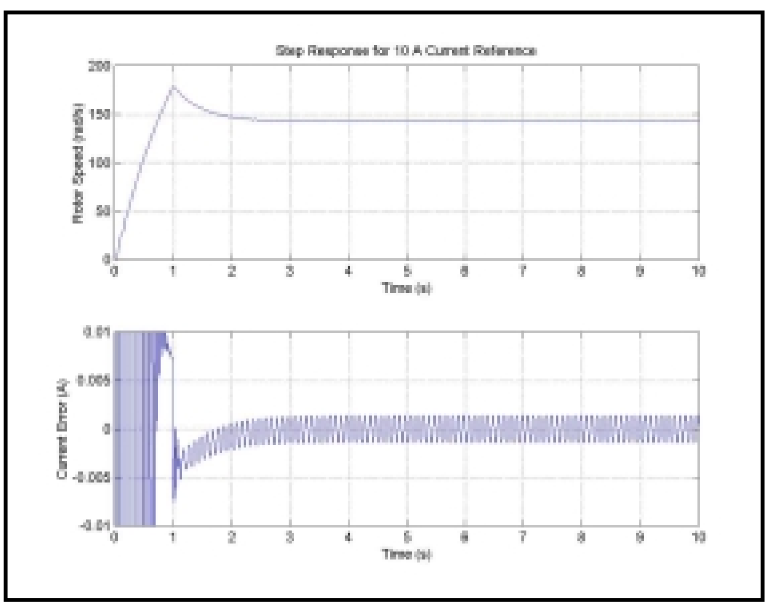

Figure 3. Step response for current controller with 10A reference.

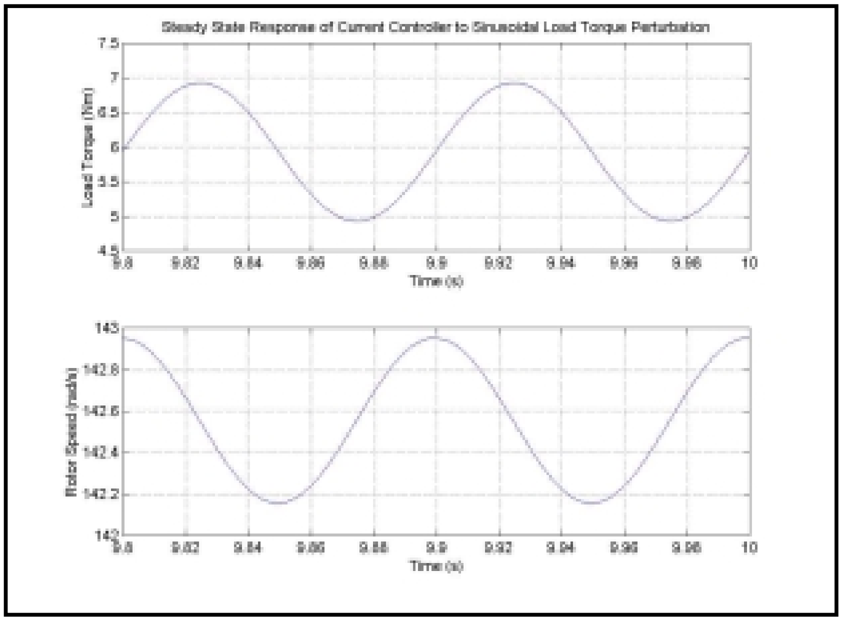

Figure 4. Steady-state response to load torque perturbation.

5 Implementation

An example of a system where DC current control can greatly improve the performance of a motor controller can be found in traction systems for electric vehicles. Figure 5 shows the electrical system for a solar-powered electric vehicle. This particular vehicle had a speed-controlled brushless DC motor for its main drive motor. Bus current feedback was used for an outer loop to make the car easier to drive by transforming the pedal to something more closely approximating a power controller. The plot shown in Figure 6 resulted from a simple speed control algorithm applied to a speed controller for the drive motor of the solar car. Although the speed was held at a constant 50 mph, the power load varied tremendously as the car completed a lap around a closed track. The variations in power result from the variations in wind speed, slight changes in grade, and small accelerations that result from speed controller loop actions.

The plot shown in Figure 7 comes from a 40 mph on-road test with a bus current control loop around a speed-controlled motor. Although Figures 6 and 7 result from different speeds and power levels, the variation in power levels is instructive about the differences between the control methods. The DC bus current controller consistently regulates the power level to within ±3 percent of nominal, while such regulation is clearly not present in the pure speed controller.

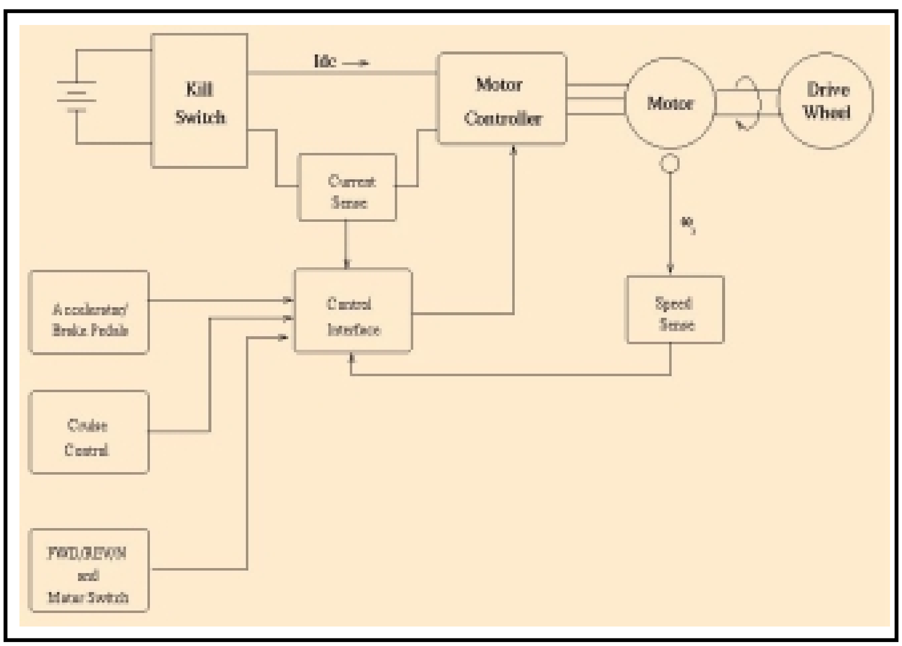

Figure 5. Solar electric vehicle drive system.

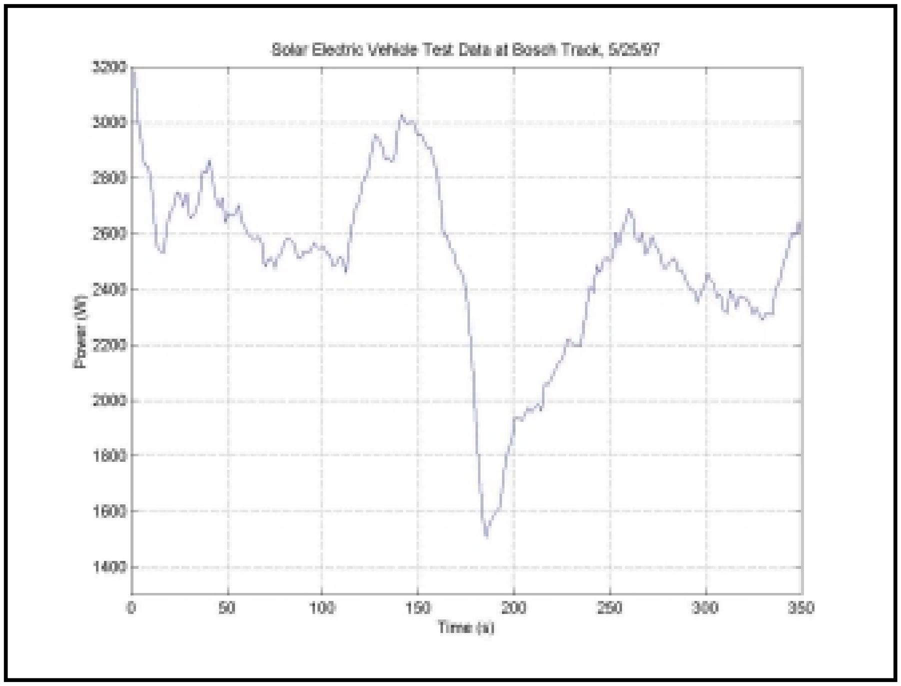

Figure 6. Solar vehicle 50 mph test without current control.

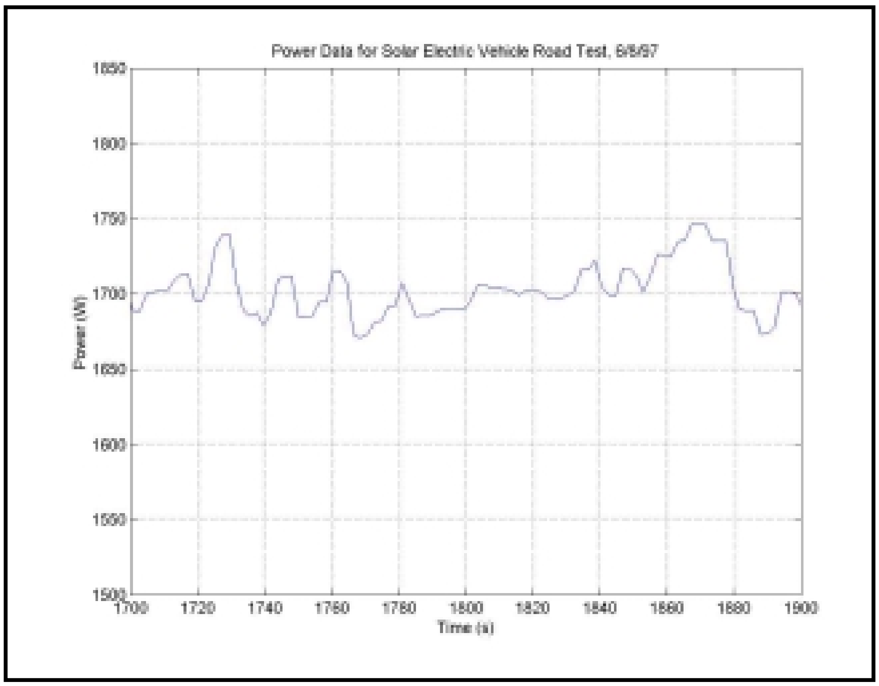

Figure 7. Solar vehicle 40 mph test with current control.

The results shown in Figure 7 represent a substantial efficiency improvement compared to those in Figure 6. Low current variation in general helps to reduce motor losses. The Figure 7 results are representative of those that can be achieved with FOC in a traction application — in a system that requires no tuning and in which the motor is fully interchangeable.

6 Conclusion

This work has given key results from a U.S. Army Construction Engineering Research Laboratory (CERL) funded program on induction motor active control, specifically, by presenting a type of feedback for simple motor controllers. The DC bus current, when used as a feedback variable, can effectively transform a speed controlled system to a power controlled system. In applications with high inertial loads, the method produces results similar to that of a torque controlled system (previously achieved only with FOC). Bus current feedback requires very little additional computation over scalar control if performed digitally, and can be implemented quite simply in an analog circuit. It has proved quite useful in an electric vehicle application, and should be considered for similar systems driven by a variable unknown load torque. It is especially valuable when tuning sensitivity must be eliminated, or when motor interchangeability is desired.

References

Blaschke, F., “The Principle of Field Orientation as Applied to the New Transvektor Closed-Loop Control System for Rotating-Field Machines,” *Siemens Review*, vol 34 (May 1972), pp 217-220.

DeDoncker, R.W., “Parameter Sensitivity of Indirect Universal Field-Oriented Controllers,” *IEEE Trans. Power Electronics*, vol 9, No. 4 (July 1994), pp 367-374.

Krause, P.C., *Analysis of Electric Machinery* (McGraw-Hill, New York, 1986).

Distribution

Chief of Engineers
ATTN: CEHEC-IM-LH (2)
ATTN: HECSA Mailroom (2)
ATTN: CECC-R
ATTN: CERD-L
ATTN: CERD-M

Defense Tech Info Center 22304
ATTN: DTIC-O (2)

9
9/99

REPORT DOCUMENTATION PAGE

Form Approved
OMB No. 0704-0188

1. AGENCY USE ONLY (Leave Blank)	2. REPORT DATE	3. REPORT TYPE AND DATES COVERED
	December 1999	Final

4. TITLE AND SUBTITLE
Bus Current Feedback for Motor Control

5. FUNDING NUMBERS
ILIR

6. AUTHOR(S)
Jonathan A. Locker, Philip T. Krein, and Hannon Maase

7. PERFORMING ORGANIZATION NAME(S) AND ADDRESS(ES)
U.S. Army Construction Engineering Research Laboratory (CERL)
P.O. Box 9005
Champaign, IL 61826-9005

8. PEFORMING ORGANIZATION REPORT NUMBER
ERDC/CERL TR-00-1

9. SPONSORING / MONITORING AGENCY NAME(S) AND ADDRESS(ES)
U.S. Army Construction Engineering Research Laboratory (CERL)
P.O. Box 9005
Champaign, IL 61826-9005

10. SPONSORING / MONITORING AGENCY REPORT NUMBER

9. SUPPLEMENTARY NOTES
Copies are available from the National Technical Information Service, 5385 Port Royal Road, Springfield, VA 22161

12a. DISTRIBUTION / AVAILABILITY STATEMENT
Approved for public release; distribution is unlimited.

12b. DISTRIBUTION CODE

13. ABSTRACT ***(Maximum 200 words)***

Many algorithms using nonlinear control ideas have been applied to the induction motor control problem to allow the user to control the torque, speed, or position response of a closed loop servo quite precisely. For many applications, the incremental improvement in transient torque, speed, or position response does not justify the additional computational requirements or a complicated tuning and commissioning process. A better solution would be to improve the utility of existing algorithms that may normally exhibit lower performance, but that can be extended easily. One such extension involves the use of the DC link current as a control variable in various motor control algorithms. This work examined the use of such a variable as an enhancement for scalar and vector control algorithms for the induction motor and discussed the effects of such a control on the operation of an electric vehicle.

14. SUBJECT TERMS
bus current
DC link current
algorithm
electrical engineering
motor controllers

15. NUMBER OF PAGES
24

16. PRICE CODE

17. SECURITY CLASSIFICATION OF REPORT	18. SECURITY CLASSIFICATION OF THIS PAGE	19. SECURITY CLASSIFICATION OF ABSTRACT	20. LIMITATION OF ABSTRACT
Unclassified	Unclassified	Unclassified	SAR